Identification of HLA-E Binding Mycobacterium tuberculosis-Derived Epitopes through Improved Prediction Models

Ruibal, Paula; Franken, Kees L.M.C.; van Meijgaarden, Krista E.; van Wolfswinkel, Marjolein; Derksen, Ian; Scheeren, Ferenc A.; van Veelen, Peter A.; Abeel, Thomas; Joosten, Simone A.; More Authors

Important note
To cite this publication, please use the final published version (if applicable).
Please check the document version above.

The Journal *of* Immunology

Identification of HLA-E Binding *Mycobacterium tuberculosis*–Derived Epitopes through Improved Prediction Models

This information is current as of October 20, 2022.

Paula Ruibal, Kees L. M. C. Franken, Krista E. van Meijgaarden, Marjolein van Wolfswinkel, Ian Derksen, Ferenc A. Scheeren, George M. C. Janssen, Peter A. van Veelen, Charlotte Sarfas, Andrew D. White, Sally A. Sharpe, Fabrizio Palmieri, Linda Petrone, Delia Goletti, Thomas Abeel, Tom H. M. Ottenhoff and Simone A. Joosten

---

Supplementary Material   http://www.jimmunol.org/content/suppl/2022/09/07/jimmunol.220012 2.DCSupplemental

Why *The JI*? Submit online.

- **Rapid Reviews! 30 days*** from submission to initial decision

- **No Triage!** Every submission reviewed by practicing scientists

- **Fast Publication!** 4 weeks from acceptance to publication

*average

Subscription   Information about subscribing to *The Journal of Immunology* is online at:
http://jimmunol.org/subscription

Permissions   Submit copyright permission requests at:
http://www.aai.org/About/Publications/JI/copyright.html

Email Alerts   Receive free email-alerts when new articles cite this article. Sign up at:
http://jimmunol.org/alerts

Identification of HLA-E Binding *Mycobacterium tuberculosis*–Derived Epitopes through Improved Prediction Models

Paula Ruibal,* Kees L. M. C. Franken,* Krista E. van Meijgaarden,*
Marjolein van Wolfswinkel,* Ian Derksen,[†] Ferenc A. Scheeren,[‡] George M. C. Janssen,[§]
Peter A. van Veelen,[§] Charlotte Sarfas,[¶] Andrew D. White,[¶] Sally A. Sharpe,[¶]
Fabrizio Palmieri,[‖] Linda Petrone,[‖] Delia Goletti,[‖] Thomas Abeel,[#,**] Tom H. M. Ottenhoff,*
and Simone A. Joosten*

Tuberculosis (TB) remains one of the deadliest infectious diseases worldwide, posing great social and economic burden to affected countries. Novel vaccine approaches are needed to increase protective immunity against the causative agent *Mycobacterium tuberculosis* (Mtb) and to reduce the development of active TB disease in latently infected individuals. Donor-unrestricted T cell responses represent such novel potential vaccine targets. HLA-E-restricted T cell responses have been shown to play an important role in protection against TB and other infections, and recent studies have demonstrated that these cells can be primed in vitro. However, the identification of novel pathogen-derived HLA-E binding peptides presented by infected target cells has been limited by the lack of accurate prediction algorithms for HLA-E binding. In this study, we developed an improved HLA-E binding peptide prediction algorithm and implemented it to identify (to our knowledge) novel Mtb-derived peptides with capacity to induce CD8^{+} T cell activation and that were recognized by specific HLA-E-restricted T cells in *Mycobacterium*-exposed humans. Altogether, we present a novel algorithm for the identification of pathogen- or self-derived HLA-E-presented peptides. *The Journal of Immunology*, 2022, 209: 1–11.

Despite the extensive administration of the century-old *Mycobacterium bovis* bacille Calmette Guérin (BCG) vaccine, 10 million new tuberculosis (TB) cases were diagnosed and 1.4 million deaths occurred as a consequence of the disease in 2019, greatly impacting the affected communities (1). The design of novel vaccine strategies to improve protection against *Mycobacterium tuberculosis* (Mtb) infection or TB disease progression in adolescents and adults, where BCG-induced protection is limited, is key to eliminating this widespread disease.

Targeting donor-unrestricted T cells is among the investigated strategies aimed at improving vaccine-induced immune protection against Mtb (2, 3). HLA-E is a nonpolymorphic HLA molecule for which two variants, HLA-E*01:01 and HLA-E*01:03, with one amino acid difference outside of the peptide binding groove, have a combined frequency distribution of more than 0.99 in 97 of 104 populations studied (4). As such, Ag presentation via HLA-E has the potential of inducing a T cell response common to all individuals (5). Importantly, HLA-E-restricted T cells have been identified as potentially significant players in immunity against Mtb through

cytotoxic and suppressive functions associated with a Th2 cytokine profile, as well as B-cell activation (6, 7). In Qa-1b-deficient mice (functional homolog of HLA-E in mice) a higher susceptibility to Mtb infection than that in wild-type mice suggested a protective role for Qa-1b-restricted T cells in vivo (8). In rhesus macaques (RMs), vaccination with rhesus CMV (RhCMV) vectors expressing Mtb Ags led to significant reduction of Mtb infection and disease, a protection that was partly associated with the induction of Mamu-E (functional homolog of HLA-E in RM) and MHC class II restricted T cells (9). Similarly, RhCMV vectored vaccines expressing SIV (10) or *Plasmodium knowlesi* (11) Ags could elicit Mamu-E-restricted T cells, which were associated with increased protection in RM. Mamu-E-restricted T cells induced by RhCMV/hepatitis B virus (HBV) produced IFN-γ upon recognition of HBV-infected primary hepatocytes in vitro, underscoring the potential of MHC-E-restricted T cells as vaccine-targetable cells to increase protection against infections (12). More recently, in vitro primed HIV-specific HLA-E-restricted CD8^{+} T cells suppressed HIV-1 replication in CD4^{+} T cells in vitro, further supporting the potential for HLA-E-restricted T cells as vaccine targets (13).

---

*Department of Infectious Diseases, Leiden University Medical Center, Leiden, the Netherlands; [†]Department of Cell and Chemical Biology, Leiden University Medical Center, Leiden, the Netherlands; [‡]Department of Dermatology, Leiden University Medical Center, Leiden, the Netherlands; [§]Center for Proteomics and Metabolomics, Leiden University Medical Center, Leiden, the Netherlands; [¶]Research and Development Department, UK Health Security Agency, Salisbury, United Kingdom; [‖]National Institute for Infectious Diseases Lazzaro Spallanzani Scientific Institute for Research, Hospitalization and Healthcare, Rome, Italy; [#]Delft Bioinformatics Lab, Delft University of Technology, Delft, the Netherlands; and **Infectious Disease and Microbiome Program, Broad Institute of MIT and Harvard, Cambridge, MA

ORCIDs: 0000-0003-3217-4497 (P.R.); 0000-0003-2818-9805 (K.E.v.M.); 0000-0003-4952-9709 (M.v.W.); 0000-0002-8304-9023 (F.A.S.); 0000-0001-9091-4030 (G.M.C.J.); 0000-0002-7898-9408 (P.A.v.V.); 0000-0001-9056-0308 (C.S.); 0000-0001-9481-0079 (A.D.W.); 0000-0001-8360-4376 (D.G.); 0000-0002-7205-7431 (T.A.); 0000-0003-3706-3403 (T.H.M.O.); 0000-0002-9878-0863 (S.A.J.).

Address correspondence and reprint requests to Dr. Simone A. Joosten, Leiden University Medical Center, Albinusdreef 2, 2333 ZA Leiden, the Netherlands. E-mail address: s.a.joosten@lumc.nl

The online version of this article contains supplemental material.

Abbreviations used in this article: β2m, β2-microglobulin; BCG, bacille Calmette Guérin; EdU, 5-ethynyl-2′-deoxyuridine; HBV, hepatitis B virus; Mtb, *Mycobacterium tuberculosis*; NHP, nonhuman primate; PPD, purified protein derivative; Rh, rhesus; RM, rhesus macaque; RT, room temperature; s/p, sample-to-positive; TB, tuberculosis; TST, tuberculin skin test.

However, detailed information about the epitopes that could potentially induce these donor-unrestricted T cell responses are poorly defined, making them difficult to identify.

Prediction of HLA-E binding peptides is limited by the lack of available binding data that inform prediction software. We recently used a newly developed high-throughput HLA-E/peptide binding assay (14) to investigate in detail the MHC-E binding motif by testing binding of a large set of peptides in the context of human, non-human primate (NHP), and mouse MHC-E molecules (15). Here, we used that knowledge to build and further improve an artificial neural networks model (16) for the prediction of HLA-E binding peptides that are Mtb derived. Peptide candidates were downselected on the basis of their binding capacity to MHC-E molecules and their conservation across Mtb genomes to ensure we selected peptides that would be relevant to most circulating Mtb strains. In addition, we selected peptides also present in the BCG genome with the idea of potentially inducing a BCG-boosting response that could increase its efficacy in poorly protected populations. Altogether, we could identify a new collection of HLA-E binding Mtb-derived peptides, some of which were recognized by specific CD8^{+} T cells. Further phenotypical and functional analyses of these HLA-E-restricted Mtb-specific CD8^{+} T cells are underway to define their potential role in protective immunity.

Materials and Methods

Generation of HLA-E binding motif models and prediction of HLA-E binding Mtb-derived peptides

Sequences and binding affinities from previously measured peptides (15) were used as training data to generate an initial artificial neural network model using NNAlign-2.1 (https://services.healthtech.dtu.dk/service.php?NNAlign-2.0) (16). On the basis of these, NNAlign calculated a sequence alignment and produced a binding motif of the peptide–MHC-E interaction, as well as a model that was subsequently used to scan the Mtb H37Rv (GenBank accession number CP003248.2; https://www.ncbi.nlm.nih.gov/nuccore/CP003248.2) proteome for the binding motif. This process was reiterated and performed in three subsequent rounds of binding prediction and testing, each with an increased training data based on sequences and sample-to-positive (s/p) ratios from newly predicted and tested peptides. Each model is an ensemble of 50 networks, each trained on one of the five cross-validation data sets with 10 hidden neurons. Each model was trained for 500 cycles, and the peptide binding core length was set to 9 aa. Final models are available upon request.

Preparation of monomers for UV-mediated exchange

Peptides were purchased from Peptide 2.0 Inc. (Chantilly, VA). Recombinant extracellular HLA-E*01:01, HLA-E*01:03, Mamu-E consensus sequence (91% sequence identity compared with HLA-E), and Qa-1[b] (85.5% sequence identity compared with HLA-E) heavy chains with a C-terminal BirA recognition site and human β2-microglobulin (β2m) were overexpressed in *Escherichia coli* and stored as described previously (15). Monomers were made by folding 2.5 mg of heavy chain solubilized in 8 M urea with 1.2 mg of prefolded β2m and 3 mg UV-sensitive peptide (VMAPJTLVL, where J is DNP amino acid) in 50 ml folding buffer (400 mM L-arginine, 0.5 mM oxidized glutathione, 5 mM reduced glutathione, 2 mM EDTA, 100 mM Tris·HCl, pH 8, glycerol 5%, and half a tablet of protease inhibitor mixture [cOmplete, Roche]). Folded monomers were concentrated on a 30 kDa filter (Amicon Ultracel 15), and Mamu-E and Qa-1[b] monomers were biotinylated using the BirA enzyme. HLA-E*01:01 and HLA-E*01:03 monomers were not biotinylated. Monomers were purified by gel filtration on a HiLoad 16/60 Superdex 75 prep grade (GE Healthcare) and stored in small aliquots with 16% of glycerol in PBS at −80°C.

UV-mediated peptide exchange reaction and detection by sandwich ELISA

UV-mediated peptide exchange and detection were performed as described previously (14, 15). Briefly, 0.5 μM of UV-sensitive MHC-E monomer was incubated in the presence of 100 μM exchange peptide in 25 μl exchange buffer (20 mM Tris [pH 7.4] and 150 mM NaCl). Exposure to UV light >350 nm for 60 min at 4°C triggered the UV-mediated peptide exchange reaction. pCMV (VLAPRTLLL), because of its known high binding capacity to MHC-E, was used as a positive control exchange peptide. As a negative control, no peptide was added to the reaction. The exchange reaction was

performed in duplicate in polypropylene U-bottomed 96-well plates (Greiner Bio-One). Detection and quantification of peptide exchange in HLA-E*01:01 and HLA-E*01:03 were performed in 96-well half-area ELISA microplates (Greiner Bio-One) coated with 10 μg/ml of purified anti-human HLA-E Ab (clone 3D12; BioLegend). Peptide exchange in previously biotinylated Mamu-E and Qa-1[b] was detected and quantified in 96-well Nunc MaxiSorp plates (Invitrogen) coated with 2 μg/ml streptavidin (Invitrogen). Coated plates were blocked with 2% IgG-free BSA in PBS and washed with 0.05% Tween 20 in PBS. Exchanged monomers were diluted 1:100 in blocking buffer and added to the wells. β2m-associated complexes were detected using 2 μg/ml HRP-conjugated anti-β2m Ab (Thermo Fisher Scientific) and amplified using a 1:15 dilution of HRP-coupled goat anti-rabbit IgG (Dako). HRP signal was developed with tetramethylbenzidine substrate (Invitrogen) and H2SO4 stop solution. Absorbance readings were obtained at 450 nm using a SpectraMax i3× Reader. The s/p ratio was calculated by subtracting background and normalizing to positive control. The results represent mean values of at least two independent experiments. For each allele, we obtained the SD for all peptide measurements (at least two per peptide) and subsequently estimated a threshold for defining binding peptides by calculating the mean (SD) (SD ≤ s/p ratio ≤ 2 × SD). We also used two times the mean SD to estimate strong binders in the context of each MHC-E allele individually (s/p ratio ≥ 2 × SD) (15).

Mtb peptide sequence conservation analysis

The 50,000 epitopes with the highest predicted binding values were tested for sequence conservation in a collection of 48,392 Mtb whole-genome sequencing publicly available data sets. Identifiers for all data sets are available upon request. Samples were aligned and processed as previously described (17). The variant calls of the 48,392 strains were used to construct a conservation profile of the complete Mtb genome, which was used to determine the conservation score S of epitope e, defined as $S(e) = C_{match}/(C_{variant} + C_{match})$, with C_{match} corresponding to the sum of matching alleles across all positions within the epitope across all samples and $C_{variant}$ the total number of mismatching alleles across all positions across all samples, both calculated when the epitope is aligned to the reference profile.

PBMC isolation

PBMCs were obtained from anonymous buffy coats from healthy adult Dutch blood bank donors who consented to scientific use of blood products. PBMCs were isolated by density centrifugation and used immediately or stored in liquid nitrogen. Donors were genotyped for HLA-E and HLA-A2, and HLA-A2 negative donors were used for all experiments.

T cell proliferation assay and flow cytometry

T cell proliferation in response to HLA-E binding peptides was assessed with the Click-iT Plus 5-ethynyl-2′-deoxyuridine (EdU) flow cytometry assay kit (Invitrogen) following the manufacturer's instructions. Briefly, $0.2 × 10^6$ PBMCs/well were cultured for 10 d in 96-well round-bottomed culture plates in the presence of 10 μg/ml peptides or control stimuli. Each condition included six replicates and medium (IMDM, 10% human serum with 10 ng/ml IL-7) without stimuli was used as a negative control. As a positive control, we included 2 μg/ml of PHA, 5 μg/ml of purified protein derivative (PPD), and 5 μg/ml of fusion early secretory antigenic target 10 kDa culture filtrate protein (ESAT6/CFP10). On day 5, PBMCs were restimulated with peptide or control proteins, and 100 U/ml IL-2 was added to the medium. Twenty-four hours before harvesting for FACS staining and Click-iT reaction, EdU was added to a final concentration of 25 μM. Once harvested, cells were washed with PBS, and cell surface Ags were Ab stained before fixation/permeabilization, and Click-iT reactions were subsequently performed. Fluorochrome-conjugated Abs against human CD3 (clone UCHT1, BioLegend) and CD8 (clone SK1, BioLegend) samples were acquired on an LSR Fortessa (BD Biosciences) and analyzed using FlowJo software version 10.7.1 (BD Biosciences).

Experimental animals

The animals used in this study were rhesus macaques (*Macaca mulatta*) of Indian genotype and obtained from an established, closed UK breeding colony (UK Health Security Agency, Porton Down, UK). Animals were housed in compatible social groups in accordance with the Home Office (UK) Code of Practice for the Housing and Care of Animals Bred, Supplied or Used for Scientific Purposes (2014) and the National Committee for Refinement, Reduction and Replacement Guidelines on Primate Accommodation, Care and Use (August 2006). Enrichment was afforded by the provision of high-level observation balconies, swings, deep litter to allow foraging, feeding puzzles, and toys. In addition to standard old-world primate pellets, further food was provided by a selection of vegetables and fruit. Animals were sedated by i.m. injection of ketamine hydrochloride (Ketaset, 100 mg/ml, 10 mg/kg; Fort Dodge Animal Health Ltd., Southampton, UK) for procedures requiring removal from their

housing. The study design and procedures were approved by the UK Health Security Agency, Porton Down Animal Welfare and Ethical Review Body, and authorized under an appropriate UK Home Office project license.

BCG vaccination

Macaques were vaccinated intradermally in the upper left arm with 100 μl BCG Danish strain 1331 (Serum Statens Institute, Copenhagen, Denmark). BCG was prepared and administered according to the manufacturer's instructions for preparation of vaccine for administration to human adults by addition of 1 ml Saunton's diluent to a vial of vaccine to give a suspension of BCG at an estimated concentration of $2–8 \times 10^6$ CFU/ml.

Blood sample collection and PBMC isolation

Macaques were sedated for blood sample collection. Blood for use in immunological analysis was collected from the femoral vein using a needle and syringe and dispensed into tubes containing heparin (Sigma-Aldrich, Gillingham, UK). PBMCs were isolated from heparin anticoagulated blood using standard methods and stored at $-196°C$ for further analysis.

Tetramer staining of PBMCs from BCG-vaccinated NHPs

Cryopreserved PBMCs from BCG-vaccinated NHPs were thawed in RPMI with 50% FCS and plated at a concentration of 3×10^6 cells/well in a 24-well plate for 2–4 h for monocyte plastic adhesion. Nonadherent cells were collected and stained with a 1:800 dilution of viability dye (Thermo Fisher Scientific) for 10 min at 4°C. Cells were washed once with FACS buffer (PBS with 0.1% BSA) and divided to be stained with a 1:50 dilution of different tetramers for 15 min at 37°C. HLA-E tetramers were produced, and peptide loading was confirmed by mass spectrometry as described previously (18, 19). Abs for CD3 (clone SP34-2, BD Biosciences) and CD8 (clone RPA-T8, BD Biosciences) staining were added and incubated for 30 min at 4°C. Cells were washed once as before, fixed with 1% paraformaldehyde, and immediately acquired on a FACSLyric (BD Biosciences). All data were analyzed using FlowJo software version 10.7.1 (BD Biosciences).

Active TB human samples

This study was approved by the ethics committee of "L. Spallanzani" National Institute of Infectious Diseases, Scientific Institute for Research, Hospitalization and Healthcare (approval number 72/2015). Written informed consent was required to participate in the study conducted at "L. Spallanzani" National Institute of Infectious Diseases. We prospectively enrolled HIV-uninfected subjects with pulmonary active TB between September 2016 and October 2019. Active TB was microbiologically diagnosed and confirmed using sputum cells by culture testing and/or nucleic acid tests (20). Patients with active TB were enrolled within 7 d of starting the specific TB treatment (T0) and at 2 mo after treatment start and at the end of therapy (between 6 and 9 mo, depending on the clinical characteristics). Human PBMCs were isolated, frozen, and stored in liquid nitrogen until use.

Tetramer staining of PBMCs from human donors

We used tuberculin skin test (TST)-positive donor PBMCs cryopreserved during a previous study comparing different immunological tests in detecting latent TB infection in the Netherlands, a low endemic country (METC project no. P07.048) (21). PBMCs were thawed in RPMI with 50% FCS and simultaneously stained and blocked with 100 μl solution containing a 1:800 dilution of viability dye (Thermo Fisher) and 1:500 dilution of purified mouse anti-human CD94 Ab (clone HP-3D9, BD Biosciences) for 30 min at room temperature (RT). Cells were washed once with FACS buffer (PBS with 0.1% BSA) and blocked with FACS buffer containing 5% human serum for 10 min at RT. After another washing step, cells were stained with a 1:50 dilution of tetramer for 30 min at 37°C in the dark. After washing, cells were fixated with 1% paraformaldehyde for 10 min at RT and then washed again. Cells were then further stained with anti-CD3 (clone UCHT1, BioLegend) and anti-CD8a (clone HIT8a, BioLegend) in 100 μl FACS buffer for 15 min at 4°C in the dark. After another wash, cells were fixated with 1% paraformaldehyde and acquired using an LSRFortessa (BD Biosciences) or a 5L CytekAurora (Cytek Biosciences, Fremont, CA). Data were analyzed using FlowJo software version 10.7.1 or the OMIQ analysis software (www.omiq.ai).

Luminex assay

PBMCs (2.5×10^5 cells/well) were cultured in duplicate wells in the presence of medium (as unstimulated control), 5 μg/ml PPD (Serum Statens Institute, Copenhagen, Denmark), or 2 μg/ml per peptide (MTBHLAE_093, MTBHLAE_031, MTBHLAE_034, and MTBHLAE_063) in a peptide pool (Peptide 2.0 Inc., Chantilly, VA) in IMDM (Life Technologies/Thermo Fisher, Bleiswijk, the Netherlands) with 10% pooled human serum (Sigma-Aldrich/Merck Live Science NV, Amsterdam, the Netherlands) in a 96-well

round-bottomed plate in a 37°C humidified CO_2 incubator. After 6 d, supernatants were harvested and stored at $-20°C$ upon further analysis. A 48-plex cytokine screening panel (Bio-Rad Laboratories, Veenendaal, the Netherlands) was performed according to the manufacturer's instructions to determine the cytokine levels in the samples. Samples were acquired on a Luminex 200 system with BioPlex manager software (version 6.1).

Thermal exchange tetramer and staining of NKG2A/CD94-expressing cells

A thermal-mediated peptide exchange reaction on monomers or multimers was performed in PCR tubes containing 10 μl of 0.5 μM multimers in the presence of 50 μM exchange peptide (P. Ruibal, I. Derksen, M. van Wolkswinkel, L. Voogd, K.L.M.C. Kranken, A.F. El Hebieshy, T. van Hall, T.A.W. Schoufour, R.H. Wijdeven, T.H.M. Ottenhoff, F.A. Scheeren, and S.A. Joosten, submitted for publication). The thermal-mediated peptide exchange reaction was triggered by incubation at 30°C for 1 h using a thermocycler. NKG2A/CD94- and LILRB1-expressing K562 cells, as well as control K562 cells, were stained with 25 μl of a 1:4 dilution of thermal exchange tetramer for 30 min at 37°C. After washing, cells were fixed with 1% paraformaldehyde and acquired on a FACSLyric (BD Biosciences). All data were analyzed using FlowJo software version 10.7.2.

Results

Improved prediction of novel Mtb-derived HLA-E binding epitopes

Our strategy to broaden our understanding of peptide binding to HLA-E included implementing a recently published high-throughput HLA-E peptide binding assay based on UV-mediated peptide exchange to obtain binding data on a large set of peptides (14). We used NNAlign to generate artificial neural network models based on the available binding data and to define an optimized peptide binding motif for prediction of HLA-E binding peptides in the Mtb genome (H37Rv) (16). We then selected predicted HLA-E binding peptides for synthesis and testing of HLA-E binding using the same binding assay described above. We fed binding data obtained by us into the training of our model to improve its predictive capacity, a cycle we performed three times before selecting the most promising peptide sequences for downstream testing on functional assays for T cell recognition (Fig. 1). We followed this strategy independently for HLA-E*01:03 and HLA-E*01:01 and thus obtained a final model for each molecule. The logos depicted represent the obtained final binding motifs for HLA-E*01:03 and HLA-E*01:01, illustrating nonameric peptide sequences that are predicted to be more relevant for binding to HLA-E molecules, based on our binding training data (Fig. 2). Taller positions and larger letter residues indicate those most relevant for binding, whereas shorter positions suggest a larger variation in the residues that are involved in HLA-E binding. These models confirm the preference for hydrophobic residues (black) in main anchor peptide positions 2 and 9, as well as secondary anchor position 7, where the rigid Pro is frequent, as was shown in previous studies (15, 22, 23).

Iterative optimization of the HLA-E/peptide binding motif led to improved predictive power for HLA-E binding peptides

All HLA-E/peptide binding assays were performed following the UV-mediated peptide exchange reaction and detection with ELISA (14, 15). Initially, we constructed an HLA-E/peptide binding model using binding data from 153 peptide sequences previously identified as HLA-E binders in humans (6, 24) and Mamu-E binders in RMs (10, 25). Surprisingly, within the first prediction set we obtained, some of our known high HLA-E binding control peptide sequences (i.e., Mtb44) were not predicted among the highest binders. Therefore, we selected 29 predicted binding peptides between the highest (position 1 in prediction set) and moderate binding values similar to Mtb44 (position 57 in prediction set), and we tested them for binding with the UV-mediated peptide exchange binding assay. Only a subset of peptides showed real binding: 12 bound HLA-E*01:01,
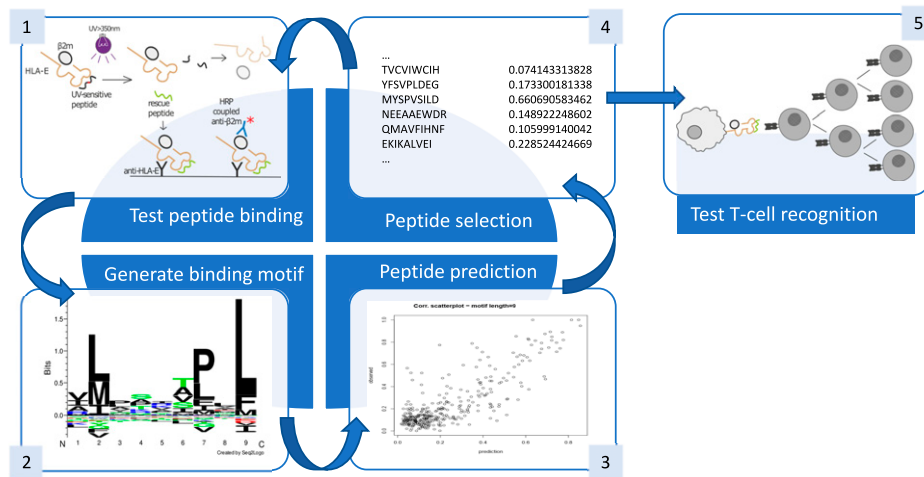
FIGURE 1. Strategy for the prediction and evaluation of (to our knowledge) novel HLA-E binding Mtb-derived peptides. We implemented a recently published HLA-E/peptide binding assay based on UV-mediated peptide exchange reaction and detection by sandwich ELISA to obtain binding information for a large set of peptides (**1**). This binding information was used to train an artificial neural network algorithm for the generation of HLA-E/peptide binding motifs using NNAlign (**2**). Peptide binding motifs were used to scan whole Mtb genomes and to predict peptide sequences able to bind HLA-E (**3**). Several peptides in the prediction set were selected for synthesis and further testing in HLA-E/peptide binding assays (**4**). This cycle (1–4) was repeated three times to improve the training and prediction capacity of the model. Finally, the most interesting peptide candidates were selected and tested for T cell recognition in stimulation assays (**5**).

6 bound HLA-E*01:03, 15 bound Mamu-E, and 11 bound Qa-1[b] (Fig. 3A, left). We extended our training data to 235 peptide sequences by including these new results, and, in addition, we included data obtained from previously published Qa-1[b] binding peptides (26, 27), as well as alanine substitutions of strong and moderate binders, into the model (15). This second prediction set more accurately predicted all our high binding controls as high binders. Here, excluding previously tested peptides, 32 peptides were selected among the best predicted binders, of which 26 bound HLA-E*01:01, 16 bound HLA-E*01:03, 11 bound Mamu-E, and 26 bound Qa-1[b] (Fig. 3A, middle).

Once again, we included these and additional binding data from amino acid substitutions of binding peptides (15), as well as other nonpublished peptide sequences tested in the interim, to perform a third and final round of model training and prediction that included a total of 332 different peptide sequences. We previously observed small differences in peptide binding affinity to HLA-E*01:01 and HLA-E*01:03, as well as Qa-1[b] and Mamu-E (15). Considering this, and with the aim of identifying promising HLA-E binding

peptides during this study for potential future preclinical research in animal models, during the third prediction round, we obtained an independent binding model to each of the four MHC-E molecules. Therefore, the final selection of predicted peptides for synthesis and testing was based on the binding to both HLA-E molecules, as well as for their binding to Qa-1[b] and Mamu-E, and, although HLA-E binding was prioritized, peptides that were predicted to bind to most of the molecules were selected with priority. As an additional selection criterion, we considered the conservation of all predicted peptide sequences across a large collection of more than 48,000 Mtb whole-genome sequence samples. We observed that most peptides that were predicted as HLA-E binders were highly conserved, with only a few peptides being specific for certain Mtb strains (Supplementary Fig. 1A). This analysis allowed us to confirm that select peptides were highly conserved (>0.93 conservation) and would thus be relevant in the context of infection with a greater number of Mtb strains. In addition, we only included peptides that were also conserved within the BCG genome, because identified peptides could potentially be considered as a component of a BCG boosting vaccine. From this
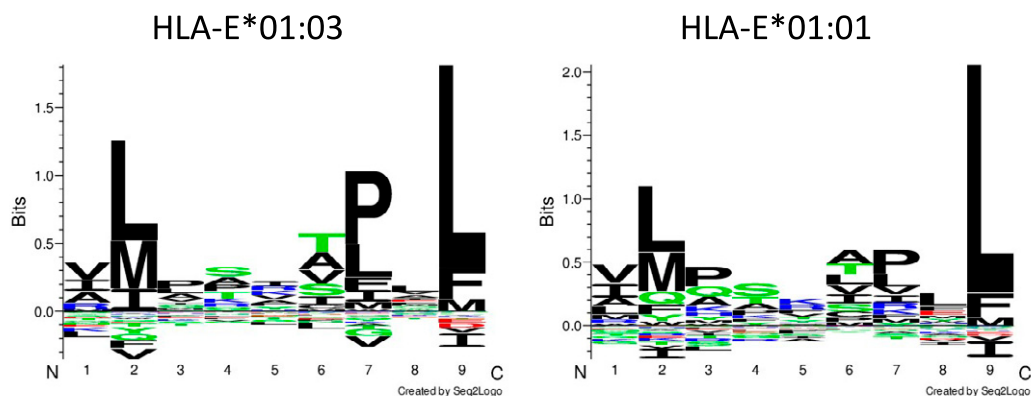
FIGURE 2. HLA-E peptide binding motifs. Logos created by Seq2Logo represent the predicted peptide binding motifs for HLA-E*01:03 (left) and HLA-E*01:01 (right) obtained after training of an artificial neural network algorithm using NNAlign. These motifs represent the nine peptide positions on the x-axis and the amount of information on the y-axis. Symbols at each position represent the amino acids, with large symbols indicating frequently observed amino acids and tall stacks representing conserved positions. These HLA-E binding motifs indicate that hydrophobic residues (black) at main anchor positions 2 and 9 are critical for peptide binding. Position 7 containing Pro or Leu is also important for peptide binding, especially for HLA-E*01:03.

FIGURE 3. Iterative rounds of prediction and testing resulted in improved prediction of (to our knowledge) novel Mtb-derived HLA-E binding peptides. (**A**) Heatmaps represent the binding affinities of the indicated peptides (rows) for the four different MHC-E molecules (columns) in three sequential rounds of peptide prediction and testing. Peptides derived from in vivo expressed (IVE)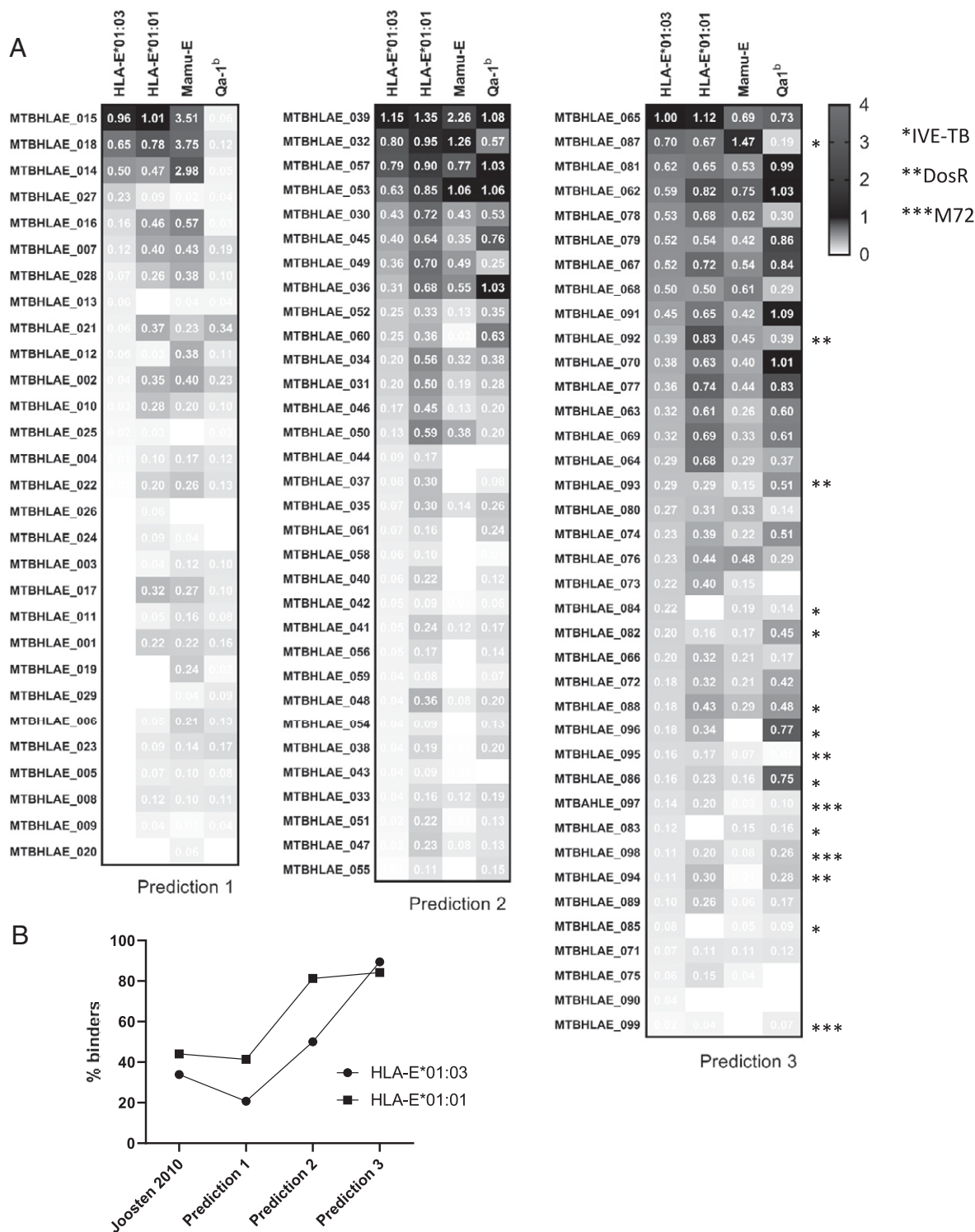 TB-, latency-, or M72-derived Ags are highlighted in the third prediction set. Numbers indicate mean values of at least two independent experiments, with white being no binding (s/p ratio = 0) and black being a binding similar to positive control (s/p ratio = 1). (**B**) The increased frequency of HLA-E binders identified in each prediction round indicates that there was a stronger predictive power with each new training model.

third round of prediction, we selected 38 peptides that were synthesized and tested for binding as before: 32 bound HLA-E*01:01, 34 bound HLA-E*01:03, 22 bound Mamu-E, and 31 bound Qa-1[b] (Fig. 3A, right). Importantly, we were interested in identifying potential HLA-E binding peptide candidates that are derived from

latency Ags (28) or that are expressed in vivo during pulmonary disease (29). In addition, we wondered whether potential HLA-E binding peptides could be identified in the M72 recombinant fusion protein vaccine candidate (30). Therefore, during the last round of prediction, we focused also on scanning these relevant Ags

with the optimized algorithm, resulting in a few predicted peptides (Fig. 3A, right).

Remarkably, we observed an improvement in the prediction power of our model over each round, as indicated by the increased frequency of identified HLA-E*01:01 and HLA-E*01:03 binders from 41% and 20%, respectively, in the first prediction to 84% and 89% in the last prediction (Fig. 3B). These results indicate that the iterative strategy of testing peptide binding, generating a binding motif, and predicting new peptides resulted in an increased prediction capacity that could possibly be improved even further when additional rounds are performed. In line with our previous observations, peptide binding to HLA-E*01:01 appears generally higher than binding to HLA-E*01:03. This may be due to the known higher stability of HLA-E*01:03 than of HLA-E*01:01, which might lead to a less efficient peptide exchange after cleavage of the UV-sensitive peptide loaded on HLA-E*01:03 (15). An overview of all tested peptides with their corresponding predictive and tested binding is available in Supplementary Table I.

T cell recognition of novel identified HLA-E binding peptides

The selection of HLA-E binding peptides that could be of interest as potential vaccine components against Mtb infection hinges on

their capacity to induce protective T cell responses. We first tested T cell recognition of predicted Mtb-derived HLA-E binding peptides by stimulating PBMCs from eight healthy Dutch blood bank donors and measuring T cell proliferation through the fluorescence detection of DNA synthesis by EdU incorporation and Click-iT chemistry (Fig. 4A). In previous studies, we observed that T cell recognition did not always correlate with high HLA-E/peptide binding (6), so here we were interested in testing T cell recognition of high as well as medium/low HLA-E binding peptides. To test a large number of peptides and optimize the identification of relevant candidates based on T cell recognition, we performed an initial screening phase using overlapping peptide pools containing the top peptides from prediction round 1 and all predicted peptides from rounds 2 and 3 (Supplemental Fig. 1B), allowing us to identify the most promising peptides as those that were common among the peptide pools associated with increased T cell proliferation. Our results showed that pools of peptides predicted during the third round led to increased T cell proliferation compared with pools of peptides predicted in previous rounds, in line with an improved HLA-E binding, potentially leading to improved T cell recognition (Supplemental Fig. 2A). In particular, peptide pools V1 and H6 were associated with higher proliferative responses in the tested donors, leading to the selection of
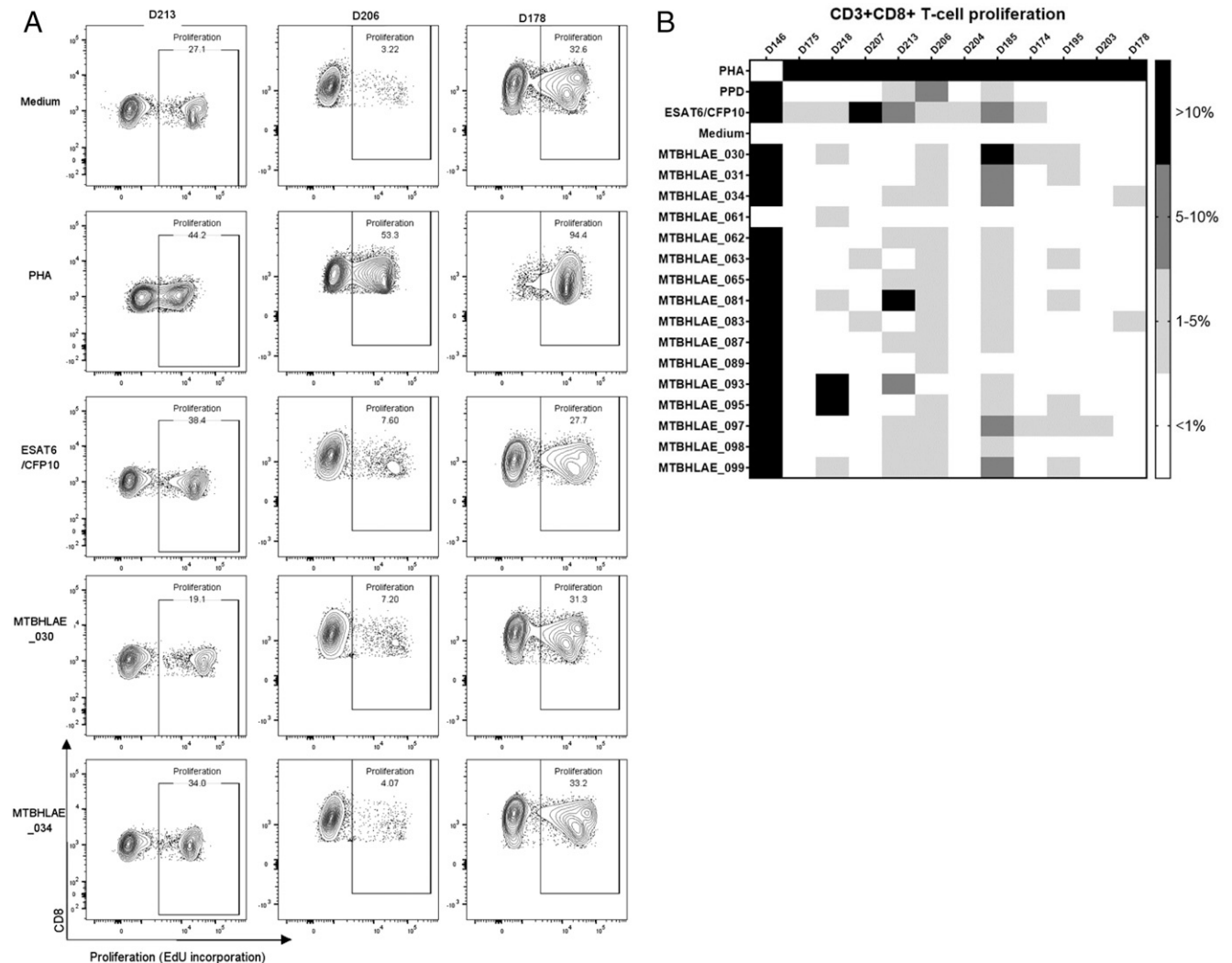
FIGURE 4. HLA-E–restricted CD8^{+} T cells from healthy donors recognize newly predicted Mtb-derived peptides. (**A**) Peptide recognition was quantified by measuring CD8^{+} T cell proliferation based on EdU incorporation after stimulation of PBMCs in the presence of peptides. FACS plots represent three representative donors (columns) and stimulation conditions (rows). (**B**) An overview of all donors (columns) and stimulation conditions (rows) tested are represented in the heatmap. Proliferation was calculated by subtracting the medium control, and results were categorized over the indicated grayscale.

peptides MTBHLAE_030, MTBHLAE_031, MTBHLAE_034, and MTBHLAE_061. In addition, peptide pools V7, V12, H8, and H10 were associated with proliferation greater than 5% in four of eight tested donors, leading to the selection of peptides MTBHLAE_062, MTBHLAE_063, MTBHLAE_065, MTBHLAE_081, MTBHL-AE_083, MTBHLAE_087, MTBHLAE_089, MTBHLAE_093, and MTBHLAE_095. To avoid an unwanted response to self in the context of a vaccine containing these peptides, we confirmed the lack of significant identity with the human genome. Finally, peptides MTBHLAE_097, MTBHLAE_098, and MTBHLAE_099 from peptide pool M72 were also selected because they were associated with T cell proliferation of two of the tested donors (Table I).

Having selected the most promising peptides, we then screened these individually in a second round of experiments and measured induced CD3$^+$CD8$^+$ T cell proliferation in peptide-stimulated PBMCs from 12 healthy Dutch donors (Fig. 4B). T cell proliferation was determined as the frequency of cells labeled with Click-iT EdU after background (medium) subtraction. Because this screening was performed using PBMCs from healthy donors from a nonendemic TB area (the Netherlands), T cell recognition was determined when proliferation was greater than 5%. To identify possible *Mycobacterium* reactivity among these donors, we used stimulation with mycobacterial PPD and ESAT6/CFP10, known Mtb-specific Ags. Our results show considerable interindividual variation in peptide recognition with no evident preference or pattern of recognition across donors. Three of five *Mycobacterium*-reactive donors showed CD3$^+$CD8$^+$ T cell reactivity to Mtb-derived peptides (proliferation >5%; Fig. 4B), whereas six of seven nonreactive donors recognized none of the tested peptides (proliferation <5%; Fig. 4B). Donors' CD3$^+$CD8$^+$ T cells recognized a wide range of 0–15 peptides, whereas 15 of 16 peptides were recognized by at least one *Mycobacterium* responder (Fig. 4B). Six of sixteen peptides were recognized by CD3$^+$CD8$^+$ T cells from at least two donors, and one peptide (MTBHLAE_093) was recognized by three independent donors (Fig. 4B). Altogether, these results suggest that predicted HLA-E binding Mtb-derived peptides are recognized by T cells in healthy Dutch blood bank donors possibly exposed to (nontuberculous) mycobacteria, as indicated by the higher number of peptides inducing proliferation in PPD-responsive donors.

HLA-E binding Mtb-derived peptides are not recognized by NKG2A/CD94

Because of the dual role of HLA-E-presented peptides in inducing T cell responses via TCR recognition as well as regulating NK cell–mediated cytotoxicity via NKG2A/CD94 signaling (31), we next tested whether the newly predicted Mtb-derived HLA-E binding peptides that we tested individually for T cell proliferation could also bind NKG2A/CD94. For this experiment, we used thermal exchange HLA-E tetramers, which we recently developed, to easily load our test peptides onto HLA-E tetramers, and we tested staining of NKG2A/CD94-expressing K562 cells (18). As a control for the proper refolding of HLA-E tetramers, we additionally stained LILRB1-expressing K562 cells because LILRB1 binds the conserved β2M and α3 domains of HLA-I molecules, regardless of the peptide bound (18, 32, 33). Our LILRB1 staining results indicated that thermal exchange with all our tested peptides was successful, whereas NKG2A/CD94 staining resulted in a total lack of signal by these HLA-E tetramers, indicating that these peptides are not recognized by this inhibitory receptor (Supplementary Fig. 2B). Therefore, our predicted peptides are not expected to inhibit NK cell–mediated cytotoxicity, an effect that could reduce elimination of Mtb-infected cells (31).

Table I. Overview of selected peptides for T cell recognition experiments, including their sequence, all selection criteria, and additional information obtained for each peptide.

Peptide ID	Sequence	Tested Binding (UV Exchange ELISA)					Protein	UniProtKB	Conservation Across Mtb Genomes	Presence in BCG	NKG2A/CD94 Recognition	HLA-A*02:01 Binding Prediction (nM)	Control Peptide Tetramer Loading (Mass spectrometry)
		HLA-E*01:01	HLA-E*01:03	Mamu-E	Qa-1b								
MTBHLAE_065	ILLSRVPEL	1.00	1.12	0.69	0.73	Rv2426c	P71922	0.999621868	Yes	No	61.93	OK
* MTBHLAE_087	KLSTLTPYL	0.70	0.67	1.47	0.19	Rv2386c	P9WFX1	0.996390215	Yes	No	4.03	OK
MTBHLAE_081	VLPLAAPWL	0.62	0.65	0.53	0.99	Rv1707	O33206	0.997075399	Yes	No	333.97	OK
MTBHLAE_062	ALQSAAPWL	0.59	0.82	0.75	1.03	Rv2328	P9WIG9	0.995321688	Yes	No	45.01	OK
MTBHLAE_030	VLPKRARLL	0.43	0.72	0.43	0.53	Rv0064	P9WFL5	0.998639217	Yes	No	2,370.85	OK
MTBHLAE_063	ILAFEAPEL	0.32	0.61	0.26	0.60	Rv2676c	P9WL45	0.999316425	Yes	No	14.1	OK
** MTBHLAE_093	RLEAVVMLL	0.29	0.29	0.15	0.51	Rv1733c	P9WLS9	0.997137399	Yes	No	15.32	OK
MTBHLAE_034	LLPIKIPLI	0.20	0.56	0.32	0.38	Rv0355c	I6Y7L4	0.993326108	Yes	No	178.54	OK
MTBHLAE_031	VLPAKLILM	0.20	0.50	0.19	0.28	Rv3193c	P9WFL3	0.999741257	Yes	No	118.35	OK
** MTBHLAE_095	RLPCRTILR	0.16	0.17	0.07	0.01	Rv1733c	P9WLS9	0.997556075	Yes	No	15,683.48	Not tested
*** MTBHLAE_097	LVAAAQMWD	0.14	0.20	0.03	0.10	Rv1196	L7N675	0.999074686	Yes	No	10,029.87	Not tested
* MTBHLAE_083	RVEAVAPWL	0.12	0.00	0.15	0.16	Rv3193c	P9WFL3	0.999371514	Yes	No	2,246.8	Not tested
*** MTBHLAE_098	AVPGRVVAL	0.11	0.20	0.08	0.26	Rv0125	O07175	0.99791747	Yes	No	838.69	Not tested
*** MTBHLAE_089	RMPFSVPWT	0.10	0.26	0.06	0.17	Rv0802c	P9WQG7	0.99833452	Yes	No	5,546.66	Not tested
MTBHLAE_061	TIPAQTPVT	0.07	0.16	−0.02	0.24	Rv3350c	Q6MWX8	0.935359636	Yes	No	23,739.39	Not tested
*** MTBHLAE_099	VHIGPTAFL	0.02	0.04	−0.02	0.07	Rv0125	O07175	0.999256841	Yes	No	2,709.26	Not tested

Peptides MTBHLAE_063, MTBHLAE_093, MTBHLAE_034, MTBHLAE_031 are the final selection of (to our knowledge) novel HLA-E binding Mtb-derived peptides based on tetramer staining of PBMCs from BCG vaccinated NHP and TST positive humans. These peptides are derived from specific groups of Ags, namely the in vivo expressed TB Ags, DosR Ags, and the M72 vaccine Ag.
*IVE-TB.
**DosR.
***M72.

Cells specific for newly identified peptides can be detected in BCG-vaccinated NHPs and Mtb-exposed humans

To confirm the relevance of these peptides in vivo, we performed tetramer staining of PBMC samples from BCG-vaccinated NHPs. We selected four newly predicted Mtb-derived peptides (MTBHLAE_062, MTBHLAE_065, MTBHLAE_087, and MTBHLAE_093), based on the combination of their HLA-E binding affinity and their capacity to induce T cell proliferation. Previously described Mtb epitopes Mtb34 and Mtb44 were included as controls (6). We loaded HLA-E tetramers with these peptides and used them to analyze the frequency of circulating peptide-specific MHC-E-restricted T cells in PBMCs from six BCG-vaccinated NHPs (18). In order to confirm proper loading of these predicted peptides into HLA-E tetramers, we analyzed the obtained tetramers by mass spectrometry and found that all tested peptides were correctly loaded (Table I). In order to explore the increased abundance of these MHC-E-restricted T cells at different time points after BCG vaccination, we analyzed samples before, 10 wk after, and 17–20 wk after BCG vaccination. Our results indicate that MHC-E-restricted CD8^{+} T cells specific to our selection of newly predicted Mtb-derived peptides were more abundant after vaccination with BCG, with statistically significant differences observed for MTBHLAE_065 and MTBHLAE_087, not only confirming these peptides as T cell epitopes but also suggesting an expansion of these cell populations as a result of vaccination (Fig. 5A, Supplementary Fig. 3A).

To further confirm recognition of our newly predicted peptides in samples from *Mycobacterium*-exposed humans, we performed tetramer staining analysis on PBMCs from TST-positive individuals (21). Considering the previous observation that HLA-E binding is not always the most accurate predictor of immunogenicity and proliferative responses observed to a wider range of peptides above (6), we decided to expand the panel of peptides to be tested. Therefore, we selected five additional peptides (MTBHLAE_030, MTBHLAE_031, MTBHLAE_034, MTBHLAE_063, MTBHLAE_081) primarily on the basis of their capacity to induce HLA-E-restricted T cell proliferation. Peptides MTBHLAE_061, MTBHLAE_083, and MTBHLAE_099 were selected on the basis of their capacity to induce T cell proliferation; however, their lower HLA-E binding capacity led to poor-quality tetramer production, and therefore these were excluded from the staining panel. Interestingly, our results showed that three of five peptides from this second selection had increased frequency of specific HLA-E-restricted CD8^{+} T cells (Fig. 5B, dark gray), compared with one of four peptides from the first selection also tested in NHPs (Fig. 5B, light gray; Supplementary Fig. 3B). Altogether, these results pinpoint HLA-E binding Mtb-derived peptides MTBHLAE_093, MTBHLAE_031, MTBHLAE_034, and MTBHLAE_063 as relevant CD8^{+} T cell epitopes, based on their capacity to induce CD8^{+} T cell proliferation and the frequency of HLA-E-restricted T cells stained with tetramers.

Previous studies have shown that HLA-E-restricted T cells that control intracellular Mtb growth in vitro can have diverse phenotypes, including cytotoxic and suppressive functions as well as expressing Th2-like cytokines (6, 7). PBMCs from patients with active TB, including longitudinal sampling from TB diagnostics until the end of TB treatment, were used for tetramer staining and peptide stimulation. Tetramer staining with MTBHLAE_031 and MBTHLAE_093 was performed; only two tetramers were used because of limited cell availability. Tetramer staining showed an abundant frequency of peptide-specific HLA-E-restricted CD8^{+} T cells at the time of TB diagnostics, suggesting high recognition of our selected peptides. Interestingly, we observed modified frequency of peptide-specific HLA-E-restricted CD8^{+} T cells over the course of treatment with 8 of 15 patients showing reduced frequency and 2 of 15 patients showing

increased frequency over time (Fig. 5C, Supplementary Fig. 3C). PBMCs stimulated with a pool of four peptides (MTBHLAE_093, MTBHLAE_031, MTBHLAE_034, and MTBHLAE_063) for 6 d secreted a large array of different cytokines and chemokines (Fig. 5D). Despite expression of several inflammatory markers, such as RANTES, MCP-1, and IL-9, in many samples, we could not detect any consistent expression of specific Th1-associated cytokines. Interestingly, we observed expression of Th2 or regulatory-like cytokines IL-13 and IL-10 at the time of TB diagnosis and at the end of treatment, respectively. Altogether, these data underscore the unorthodox phenotype that has been associated with HLA-E-restricted T cell responses and warrants a deeper functional analysis in a larger collection of samples.

Discussion

Several studies have shown that HLA-E-restricted T cells have the capacity to improve protection against infectious agents such as Mtb (7–9), SIV/HIV (10), HBV (12), and *P. knowlesi* (11). These T cell responses can be an interesting target for vaccination because of the nonpolymorphic nature of the HLA-E Ag-presenting molecule, which has the potential to induce a similar response in all individuals (5). Further supporting the potential of these unconventional T cells as vaccine targets, HIV-specific HLA-E-restricted CD8^{+} T cells could be primed in vitro, leading to the suppression of HIV-1 replication in infected cells (13). However, the number of peptides described to induce such responses remains restricted, and tools to identify relevant Ags in the context of HLA-E-restricted T cell responses are limited. In this study, we implemented a high-throughput HLA-E/peptide binding assay to develop an improved peptide prediction algorithm for the identification of novel Mtb-derived HLA-E binding peptides. We tested peptide binding to HLA-E with the UV-mediated peptide exchange binding assay (14, 15) and used the results to train a neural network model for the prediction of novel HLA-E binding Mtb-derived peptides (16). Our approach to investigate HLA-E binding to larger and more diverse peptide collections differed from previous attempts to predict HLA-E binding peptides based on limited peptide libraries selectively focusing on specific anchor positions (6, 22). This greater diversity in the sequences studied is expected to increase the predictive power of alternative peptides that may not entirely follow the canonical HLA-E binding motif described. By reiterating this process through the testing of newly predicted HLA-E binding peptides, we improved our model with each round of testing and prediction, each time yielding a higher frequency of HLA-E binding peptides than in the previous round. Of note, this HLA-E binding peptide prediction algorithm can be implemented to identify peptides derived from any protein sequence, allowing the identification of peptides originating from any microorganism or mutated proteins in the case of malignancies.

Although HLA-E*01:01 and HLA-E*01:03 are extremely similar, numerous studies have demonstrated differences in peptide binding to and cell surface stability of each molecule (34–36). The single-nucleotide polymorphism between the two molecules might lead to modifications in the neighboring charges, causing, in turn, differences in peptide binding stability (15, 37). These differences may be partially explained by the small variations in amino acid preferences illustrated in the peptide binding motifs and may even have functional consequences, as hinted by increased disease risk or protection being associated with HLA-E*01:01 or HLA-E*01:03 homozygosity (38). In line with this, the selection of more than one peptide would be an interesting approach for future vaccination purposes.

Despite the importance and relevance of determining HLA-E binding affinity to predict novel peptides able to induce HLA-E-restricted T cell responses, peptide binding to HLA-E per se does
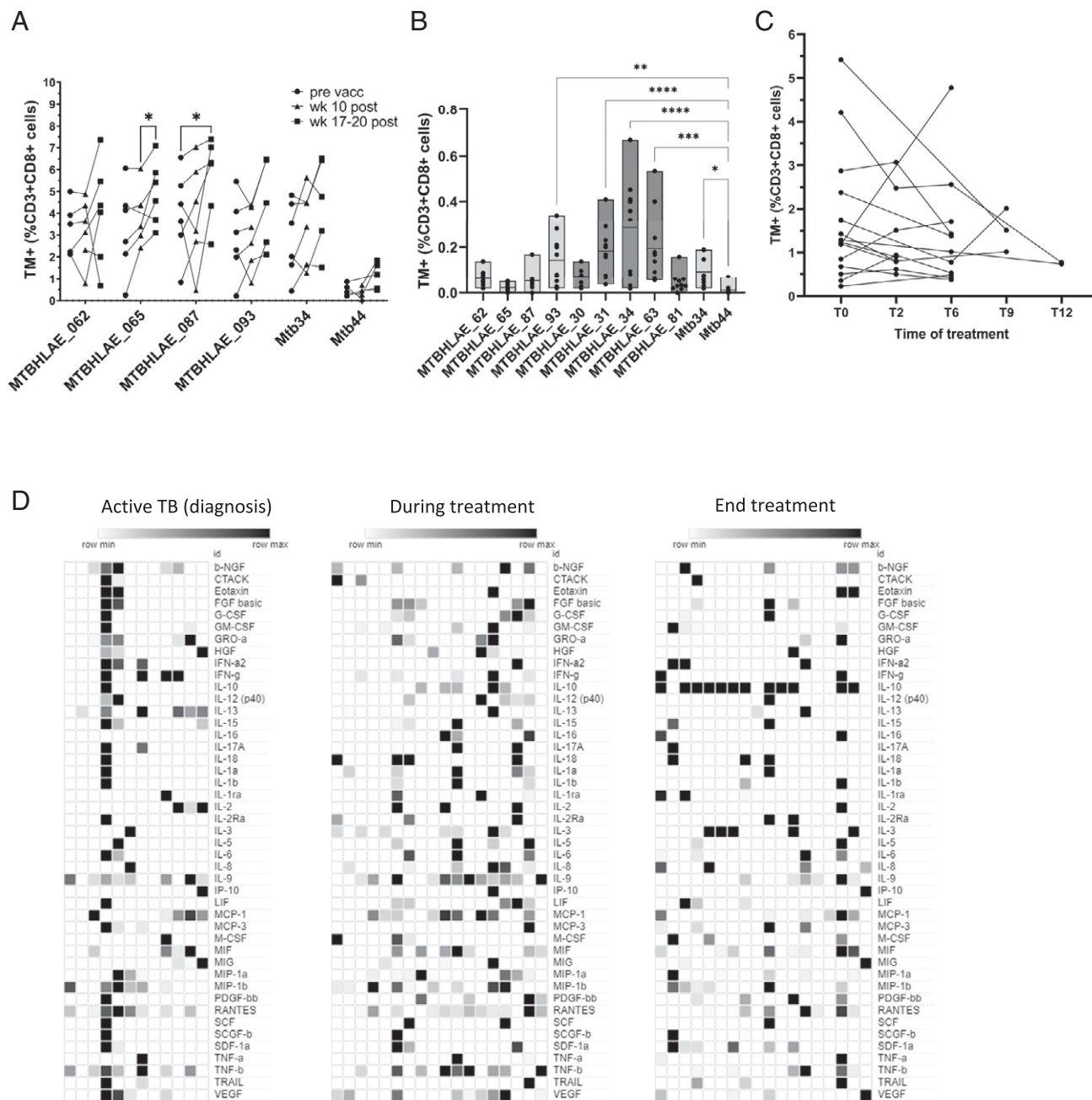
FIGURE 5. HLA-E–restricted CD8⁺ T cells specific to newly identified peptides can be detected in BCG-vaccinated NHPs and TST-positive humans. (**A**) Symbols and lines represent tetramer staining in samples obtained from six rhesus macaques before (circles), 10 wk after (triangles), and 17–20 wk after (squares) BCG vaccination. Peptides loaded in the tetramers are indicated in the x-axis labels. p Values were calculated using two-way ANOVA: *p < 0.05. (**B**) Floating bars represent tetramer staining in samples obtained from 10 TST-positive human donors. Light gray bars indicate tetramers that were also tested in the NHPs, and dark gray bars indicate tetramers that were tested only in this human sample panel. p Values were calculated using the Kruskal-Wallis test with multiple test correction: *p < 0.05, **p < 0.005, ***p < 0.001, ***p < 0.0001. (**C**) Symbols and lines represent tetramer staining with tetramers loaded with MTBHLAE_031 and MBTHLAE_093 in samples obtained from 15 patients with active TB from the time of diagnosis until the end of treatment. (**D**) Heatmaps represent secreted cytokine production upon 6-d stimulation with peptide pool (MTBHLAE_093, MTBHLAE_031, MTBHLAE_034, and MTBHLAE_063) of samples obtained from 15 patients with active TB at the time of diagnosis, during treatment, and at the end of treatment. Columns represent samples, and rows represent markers, with white being no expression and increasingly darker colors being higher expression.

not correlate with T cell recognition (6). Therefore, we tested our newly predicted peptides in T cell proliferation experiments. This allowed us to downselect peptides that, on top of being HLA-E binders, could be recognized by CD8⁺ T cells from healthy Dutch donors, suggesting they were indeed processed and presented by APCs for the induction of specific T cells. Not surprisingly, certain peptides with high HLA-E binding affinity were not recognized by T cells. This

might be explained by the possible formation of high-affinity nonstimulatory pMHC/TCR interactions limiting T cell activation (39). Alternatively, peptides might be displayed by the Ag-presenting molecule in a way that prevents "on the top" TCR binding, therefore failing to activate TCR signaling (40). This hypothesis is further supported by the lack of NKG2A/CD94 binding of these HLA-E–presented Mtb-derived peptides, which might indicate a particular

complex conformation in the presence of these high HLA-E binding peptides that restricts receptor binding. A third possibility to consider may be that peptides not recognized by T cells may simply mimic self-peptides and thus are excluded from this interaction after the negative selection of self-reactive T cells in the thymus (41). In any case, the lack of correlation between peptide/HLA-E binding and TCR recognition emphasizes the need to test T cell recognition of predicted HLA-E binding peptides under consideration for vaccine design. Our improved prediction algorithm facilitates the identification of potential pathogen- or tumor-derived peptides. Nevertheless, additional information on how newly discovered HLA-E binding peptides behave in terms of recognition by the relevant immune target cells is crucial for the optimal selection of vaccine components.

Our tetramer staining showed that three of four peptides with higher positive tetramer staining (MTBHLAE_093, MTBHLAE_031, MTBHLAE_034) were moderate HLA-E-binders and increased T cell proliferation during stimulation assays, suggesting productive TCR recognition. Conversely, high HLA-E binding peptides associated with lower tetramer staining and T cell proliferation support lack of TCR engagement rather than being involved in a nonstimulatory interaction. However, more detailed molecular dynamic simulations and structural analyses of these interactions are needed to confirm this hypothesis. HLA-E binding Mtb-derived peptides associated with positive tetramer staining do not show an obvious common sequence that could support this behavior, but they are all moderate HLA-E binders, suggesting that this could be optimal to induce productive TCR signaling. This is in line with previous studies showing that certain conformational flexibility within the peptide–MHC interactions was in turn associated with mobile TCR rearrangements promoting recognition and signaling (42, 43). Indeed, previous analyses of HLA-E binding peptide sequences identified the presence of rigid or bulky residues in central positions, which may be associated with moderate or flexible HLA-E binding and could potentially promote TCR recognition (15). Structural analyses, as well as affinity and avidity assessment, are needed to further elucidate the role of HLA-E pocket occupancy in the interactions of TCR receptors with side chains of HLA-E binding peptides composed of alternative main anchor residues.

Lampen et al. demonstrated a significant overlap between the peptide binding motifs to HLA-E and HLA-A2 (44). Therefore, an important aspect in the present study was to confirm HLA-E restriction of the peptide-specific CD8$^+$ T cell responses observed. Indeed, HLA-E tetramer staining of latently infected (TST-positive) human samples supports that the observed responses most likely occur through HLA-E-mediated Ag presentation, although cross-reactivity between HLA-E-presented peptides and HLA-A2-restricted T cell recognition cannot be fully discarded. Despite the possibility for HLA-A2 presentation (Table I), HLA class I presentation of these peptides would potentially contribute to elimination of infected cells and would not promote bacterial persistence, although consequences of this dual binding must be carefully considered (45).

Tetramer staining in BCG-vaccinated NHPs showed increased frequency of Mtb-specific MHC-E-restricted CD8$^+$ T cells after vaccination compared with the prevaccination time point, in line with an expansion of these specific cell populations in response to the vaccine. This finding is of particular interest when considering the potential of such peptides as components of a subunit booster vaccine after a BCG prime to increase protection against pulmonary tuberculosis in adolescents and adults. In accordance with this, our analysis of peptide sequence conservation across Mtb genomes ensures that the selected peptides would be relevant to induce protection against the majority of circulating strains.

The identification of novel HLA-E binding Mtb-derived peptides with the capacity to induce CD8$^+$ T cell responses could be of great value for vaccine design. Because of the dual role of HLA-E-mediated

Ag presentation in activating T cells through TCR recognition and regulating NK cells through NKG2A/CD94 recognition, we evaluated whether our selected peptides could bind this inhibitory receptor before considering their potential vaccine component candidacy (31). The selected peptides were not involved in inducing potential inhibitory signaling pathways and could thus be considered as potential subunit vaccine components. Whether these peptides are involved in the induction of HLA-E-restricted T cells with phenotypical and functional capacity to protect against Mtb infection remains to be elucidated in future studies. It will be interesting to dissect the cytokine profile of such T cell responses, because Mtb-specific HLA-E-restricted T cells have previously been associated with a dominant effector memory phenotype ex vivo and an unorthodox Th2-like response that was also associated with control of intracellular Mtb growth in vitro (7, 46). Cytotoxic responses mediated by HLA-E-restricted T cell responses were also identified in the context of *Salmonella typhimurium*, CMV, EBV, and HIV infections, further supporting the potential relevance of these immune cells as protective vaccine targets (24, 47–49).

Altogether, this study has identified (to our knowledge) novel Mtb-derived HLA-E binding peptides involved in the induction of T cell responses and opens possibilities to identify and include Mtb-derived HLA-E binding peptides in novel vaccine strategies, as a booster or complementary vaccine to BCG. Future research is necessary to further dissect the role of these peptide-specific HLA-E-restricted T cells during Mtb infection to elucidate their potential phenotype and functionality as well as their involvement in possible protective immunity against Mtb infection or TB disease.

Acknowledgments

Disclosures

The authors have no financial conflicts of interest.

References

1. World Health Organization (WHO). Global tuberculosis report 2020. Geneva, Switzerland: WHO.
2. Ruibal, P., L. Voogd, S. A. Joosten, and T. H. M. Ottenhoff. 2021. The role of donor-unrestricted T-cells, innate lymphoid cells, and NK cells in anti-mycobacterial immunity. *Immunol. Rev.* 301: 30–47.
3. Joosten, S. A., T. H. M. Ottenhoff, D. M. Lewinsohn, D. F. Hoft, D. B. Moody, and C. Seshadri; Collaboration for Tuberculosis Vaccine Discovery - Donor-Unrestricted T-cells Working Group, Bill and Melinda Gates Foundation. 2019. Harnessing donor unrestricted T-cells for new vaccines against tuberculosis. *Vaccine* 37: 3022–3030.
4. Sauter, J., K. Putke, D. Schefzyk, J. Pruschke, U. V. Solloch, S. N. Bernas, C. Massalski, K. Daniel, A. Klussmeier, J. A. Hofmann, et al. 2021. HLA-E typing of more than 2.5 million potential hematopoietic stem cell donors: methods and population-specific allele frequencies. *Hum. Immunol.* 82: 541–547.
5. Ottenhoff, T. H. M., and S. A. Joosten. 2019. Mobilizing unconventional T-cells. *Science* 366: 302–303.
6. Joosten, S. A., K. E. van Meijgaarden, P. C. van Weeren, F. Kazi, A. Geluk, N. D. L. Savage, J. W. Drijfhout, D. R. Flower, W. A. Hanekom, M. R. Klein, and T. H. M. Ottenhoff. 2010. *Mycobacterium tuberculosis* peptides presented by HLA-E molecules are targets for human CD8$^+$ T-cells with cytotoxic as well as regulatory activity. *PLoS Pathog.* 6: e1000782.
7. van Meijgaarden, K. E., M. C. Haks, N. Caccamo, F. Dieli, T. H. M. Ottenhoff, and S. A. Joosten. 2015. Human CD8$^+$ T-cells recognizing peptides from *Mycobacterium tuberculosis* (Mtb) presented by HLA-E have an unorthodox Th2-like, multifunctional, Mtb inhibitory phenotype and represent a novel human T-cell subset. *PLoS Pathog.* 11: e1004671.
8. Bian, Y., S. Shang, S. Siddiqui, J. Zhao, S. A. Joosten, T. H. M. Ottenhoff, H. Cantor, and C. R. Wang. 2017. MHC Ib molecule Qa-1 presents *Mycobacterium*

tuberculosis peptide antigens to CD8$^+$ T-cells and contributes to protection against infection. *PLoS Pathog.* 13: e1006384.

9. Hansen, S. G., D. E. Zak, G. Xu, J. C. Ford, E. E. Marshall, D. Malouli, R. M. Gilbride, C. M. Hughes, A. B. Ventura, E. Ainslie, et al. 2018. Prevention of tuberculosis in rhesus macaques by a cytomegalovirus-based vaccine. *Nat. Med.* 24: 130–143.

10. Hansen, S. G., H. L. Wu, B. J. Burwitz, C. M. Hughes, K. B. Hammond, A. B. Ventura, J. S. Reed, R. M. Gilbride, E. Ainslie, D. W. Morrow, et al. 2016. Broadly targeted CD8$^+$ T-cell responses restricted by major histocompatibility complex E. *Science* 351: 714–720.

11. Hansen, S. G., J. Womack, I. Scholz, A. Renner, K. A. Edgel, G. Xu, J. C. Ford, M. Grey, B. St Laurent, J. M. Turner, et al. 2019. Cytomegalovirus vectors expressing *Plasmodium knowlesi* antigens induce immune responses that delay parasitemia upon sporozoite challenge. *PLoS One* 14: e0210252.

12. Burwitz, B. J., P. K. Hashiguchi, M. Mansouri, C. Meyer, R. M. Gilbride, S. Biswas, J. L. Womack, J. S. Reed, H. L. Wu, M. K. Axthelm, et al. 2020. MHC-E-restricted CD8$^+$ T-cells target hepatitis B virus-infected human hepatocytes. *J. Immunol.* 204: 2169–2176.

13. Yang, H., M. Rei, S. Brackenridge, E. Brenna, H. Sun, S. Abdulhaqq, M. K. P. Liu, W. Ma, P. Kurupati, X. Xu, et al. 2021. HLA-E restricted, HIV-1 suppressing, Gag specific CD8$^+$ T-cells offer universal vaccine opportunities. *Sci. Immunol.* 6: eabg1703.

14. Walters, L. C., A. J. McMichael, and G. M. Gillespie. 2020. Detailed and atypical HLA-E peptide binding motifs revealed by a novel peptide exchange binding assay. *Eur. J. Immunol.* 50: 2075–2091.

15. Ruibal, P., K. L. M. C. Franken, K. E. van Meijgaarden, J. J. F. van Loon, D. van der Steen, H. M. Heemskerk, T. H. M. Ottenhoff, and S. A. Joosten. 2020. Peptide binding to HLA-E molecules in humans, nonhuman primates, and mice reveals unique binding peptides but remarkably conserved anchor residues. *J. Immunol.* 205: 2861–2872.

16. Nielsen, M., and M. Andreatta. 2017. NNAlign: a platform to construct and evaluate artificial neural network models of receptor-ligand interactions. *Nucleic Acids Res.* 45: W344–W349.

17. Manson, A. L., K. A. Cohen, T. Abeel, C. A. Desjardins, D. T. Armstrong, C. E. Barry III, J. Brand, S. B. Chapman, S. N. Cho, A. Gabrielian, et al.; TBResist Global Genome Consortium. 2017. Genomic analysis of globally diverse *Mycobacterium tuberculosis* strains provides insights into the emergence and spread of multidrug resistance. *Nat. Genet.* 49: 395–402.

18. Ruibal, P., K. L. M. C. Franken, K. E. van Meijgaarden, L. C. Walters, A. J. McMichael, G. M. Gillespie, S. A. Joosten, T. H. M. Ottenhoff. Discovery of HLA-E-Presented Epitopes: MHC-E/Peptide Binding and T-Cell Recognition. *Methods. Mol. Biol.* In press.

19. Luimstra, J. J., M. A. Garstka, M. C. J. Roex, A. Redeker, G. M. C. Janssen, P. A. van Veelen, R. Arens, J. H. F. Falkenburg, J. Neefjes, and H. Ovaa. 2018. A flexible MHC class I multimer loading system for large-scale detection of antigen-specific T-cells. *J. Exp. Med.* 215: 1493–1504.

20. Goletti, D., G. Delogu, A. Matteelli, and G. B. Migliori. 2022. The role of IGRA in the diagnosis of tuberculosis infection, differentiating from active tuberculosis, and decision making for initiating treatment or preventive therapy of tuberculosis infection. *Int. J. Infect. Dis.* DOI: 10.1016/j.ijid.2022.02.047.

21. de Paus, R. A., K. E. van Meijgaarden, C. Prins, M. H. Kamphorst, S. M. Arend, T. H. M. Ottenhoff, and S. A. Joosten. 2017. Immunological characterization of latent tuberculosis infection in a low endemic country. *Tuberculosis (Edinb.)* 106: 62–72.

22. Miller, J. D., D. A. Weber, C. Ibegbu, J. Pohl, J. D. Altman, and P. E. Jensen. 2003. Analysis of HLA-E peptide-binding specificity and contact residues in bound peptide required for recognition by CD94/NKG2. *J. Immunol.* 171: 1369–1375.

23. Braud, V., E. Y. Jones, and A. McMichael. 1997. The human major histocompatibility complex class Ib molecule HLA-E binds signal sequence-derived peptides with primary anchor residues at positions 2 and 9. *Eur. J. Immunol.* 27: 1164–1169.

24. Nattermann, J., H. D. Nischalke, V. Hofmeister, B. Kupfer, G. Ahlenstiel, G. Feldmann, J. Rockstroh, E. H. Weiss, T. Sauerbruch, and U. Spengler. 2005. HIV-1 infection leads to increased HLA-E expression resulting in impaired function of natural killer cells. *Antivir. Ther.* 10: 95–107.

25. Hannoun, Z., Z. Lin, S. Brackenridge, N. Kuse, T. Akahoshi, N. Borthwick, A. McMichael, H. Murakoshi, M. Takiguchi, and T. Hanke. 2018. Identification of novel HIV-1-derived HLA-E-binding peptides. *Immunol. Lett.* 202: 65–72.

26. Nagarajan, N. A., F. Gonzalez, and N. Shastri. 2012. Nonclassical MHC class Ib-restricted cytotoxic T-cells monitor antigen processing in the endoplasmic reticulum. *Nat. Immunol.* 13: 579–586.

27. Doorduijn, E. M., M. Sluijter, B. J. Querido, U. J. E. Seidel, C. C. Oliveira, S. H. van der Burg, and T. van Hall. 2018. T-cells engaging the conserved MHC class Ib molecule Qa-1b with TAP-independent peptides are semi-invariant lymphocytes. *Front. Immunol.* 9: 60.

28. Serra-Vidal, M. M., I. Latorre, K. L. Franken, J. Díaz, M. L. de Souza-Galvão, I. Casas, J. Maldonado, C. Milà, J. Solsona, M. A. Jimenez-Fuentes, et al. 2014. Immunogenicity of 60 novel latency-related antigens of *Mycobacterium tuberculosis*. *Front. Microbiol.* 5: 517.

29. Coppola, M., K. E. van Meijgaarden, K. L. M. C. Franken, S. Commandeur, G. Dolganov, I. Kramnik, G. K. Schoolnik, I. Comas, O. Lund, C. Prins, et al. 2016. New genome-wide algorithm identifies novel in-vivo expressed *Mycobacterium tuberculosis* antigens inducing human T-cell responses with classical and unconventional cytokine profiles. *Sci. Rep.* 6: 37793.

30. Tait, D. R., M. Hatherill, O. Van Der Meeren, A. M. Ginsberg, E. Van Brakel, B. Salaun, T. J. Scriba, E. J. Akite, H. M. Ayles, A. Bollaerts, et al. 2019. Final analysis of a trial of M72/AS01E vaccine to prevent tuberculosis. *N. Engl. J. Med.* 381: 2429–2439.

31. Lee, N., M. Llano, M. Carretero, A. Ishitani, F. Navarro, M. López-Botet, and D. E. Geraghty. 1998. HLA-E is a major ligand for the natural killer inhibitory receptor CD94/NKG2A. *Proc. Natl. Acad. Sci. USA* 95: 5199–5204.

32. Chapman, T. L., A. P. Heikeman, and P. J. Bjorkman. 1999. The inhibitory receptor LIR-1 uses a common binding interaction to recognize class I MHC molecules and the viral homolog UL18. *Immunity* 11: 603–613.

33. Willcox, B. E., L. M. Thomas, and P. J. Bjorkman. 2003. Crystal structure of HLA-A2 bound to LIR-1, a host and viral major histocompatibility complex receptor. *Nat. Immunol.* 4: 913–919.

34. Celik, A. A., T. Kraemer, T. Huyton, R. Blasczyk, and C. Bade-Döding. 2016. The diversity of the HLA-E-restricted peptide repertoire explains the immunological impact of the Arg107Gly mismatch. *Immunogenetics* 68: 29–41.

35. Maier, S., M. Grzeschik, E. H. Weiss, and M. Ulbrecht. 2000. Implications of HLA-E allele expression and different HLA-E ligand diversity for the regulation of NK cells. *Hum. Immunol.* 61: 1059–1065.

36. Strong, R. K., M. A. Holmes, P. Li, L. Braun, N. Lee, and D. E. Geraghty. 2003. HLA-E allelic variants. Correlating differential expression, peptide affinities, crystal structures, and thermal stabilities. *J. Biol. Chem.* 278: 5082–5090.

37. Grant, E. J., A. T. Nguyen, C. A. Lobos, C. Szeto, D. S. M. Chatzileontiadou, and S. Gras. 2020. The unconventional role of HLA-E: the road less traveled. *Mol. Immunol.* 120: 101–112.

38. Kanevskiy, L., S. Erokhina, P. Kobyzeva, M. Streltsova, A. Sapozhnikov, and E. Kovalenko. 2019. Dimorphism of HLA-E and its disease association. *Int. J. Mol. Sci.* 20: 5496.

39. Sibener, L. V., R. A. Fernandes, E. M. Kolawole, C. B. Carbone, F. Liu, D. McAffee, M. E. Birnbaum, X. Yang, L. F. Su, W. Yu, et al. 2018. Isolation of a structural mechanism for uncoupling T-cell receptor signaling from peptide-MHC binding. *Cell* 174: 672–687.e27.

40. Szeto, C., C. A. Lobos, A. T. Nguyen, and S. Gras. 2020. TCR recognition of peptide–MHC-I: rule makers and breakers. *Int. J. Mol. Sci.* 22: 68.

41. Palmer, E. 2003. Negative selection – clearing out the bad apples from the T-cell repertoire. *Nat. Rev. Immunol.* 3: 383–391.

42. Hawse, W. F., S. De, A. I. Greenwood, L. K. Nicholson, J. Zajicek, E. L. Kovrigin, D. M. Kranz, K. C. Garcia, and B. M. Baker. 2014. TCR scanning of peptide/MHC through complementary matching of receptor and ligand molecular flexibility. *J. Immunol.* 192: 2885–2891.

43. Natarajan, K., J. Jiang, N. A. May, M. G. Mage, L. F. Boyd, A. C. McShan, N. G. Sgourakis, A. Bax, and D. H. Margulies. 2018. The role of molecular flexibility in antigen presentation and T-cell receptor-mediated signaling. *Front. Immunol.* 9: 1657.

44. Lampen, M. H., C. Hassan, M. Sluijter, A. Geluk, K. Dijkman, J. M. Tjon, A. H. de Ru, S. H. van der Burg, P. A. van Veelen, and T. van Hall. 2013. Alternative peptide repertoire of HLA-E reveals a binding motif that is strikingly similar to HLA-A2. *Mol. Immunol.* 53: 126–131.

45. Sensi, M., G. Pietra, A. Molla, G. Nicolini, C. Vegetti, I. Bersani, E. Millo, E. Weiss, L. Moretta, M. C. Mingari, and A. Anichini. 2009. Peptides with dual binding specificity for HLA-A2 and HLA-E are encoded by alternatively spliced isoforms of the antioxidant enzyme peroxiredoxin 5. *Int. Immunol.* 21: 257–268.

46. Prezzemolo, T., K. E. van Meijgaarden, K. L. M. C. Franken, N. Caccamo, F. Dieli, T. H. M. Ottenhoff, and S. A. Joosten. 2018. Detailed characterization of human *Mycobacterium tuberculosis* specific HLA-E restricted CD8$^+$ T cells. *Eur. J. Immunol.* 48: 293–305.

47. Salerno-Gonçalves, R., M. Fernandez-Viña, D. M. Lewinsohn, and M. B. Sztein. 2004. Identification of a human HLA-E-restricted CD8$^+$ T-cell subset in volunteers immunized with *Salmonella enterica* serovar Typhi strain Ty21a typhoid vaccine. *J. Immunol.* 173: 5852–5862.

48. Pietra, G., C. Romagnani, P. Mazzarino, M. Falco, E. Millo, A. Moretta, L. Moretta, and M. C. Mingari. 2003. HLA-E-restricted recognition of cytomegalovirus-derived peptides by human CD8$^+$ cytolytic T lymphocytes. *Proc. Natl. Acad. Sci. USA* 100: 10896–10901.

49. Jørgensen, P. B., A. H. Livbjerg, H. J. Hansen, T. Petersen, and P. Höllsberg. 2012. Epstein-Barr virus peptide presented by HLA-E is predominantly recognized by CD8^{bright} cells in multiple sclerosis patients. *PLoS One* 7: e46120.